Integrated IR Modulator with a Quantum Cascade Laser

Janusz Mikołajczyk * 🆔 **and Dariusz Szabra**

Institute of Optoelectronics, Military University of Technology, S.Kaliskiego 2, 00908 Warsaw, Poland; dariusz.szabra@wat.edu.pl
* Correspondence: janusz.mikolajczyk@wat.edu.pl; Tel.: +48-261-839-792

Abstract: This paper presents an infrared pulsed modulator into which quantum cascade lasers and a current driver are integrated. The main goal of this study was to determine the capabilities of a new modulator design based on the results of its electrical model simulation and laboratory experiments. A simulation model is a unique tool because it includes the electrical performance of the lasing structure, signal wiring, and driving unit. In the laboratory model, a lasing structure was mounted on the interfacing poles as close to the switching electronics as possible with direct wire bonding. The radiation pulses and laser biasing voltage were registered to analyze the influence of laser module impedance. Both simulation and experimental results demonstrated that the quantum cascade laser (QC laser) design strongly influenced the shape of light, driving current, and biasing voltage pulses. It is a complex phenomenon depending on the laser construction and many other factors, e.g., the amplitude and time parameters of the supplying current pulses. However, this work presents important data to develop or modify numerical models describing QC laser operation. The integrated modulator provided pulses with a 20–100 ns duration and a frequency of 1 MHz without any active cooling. The designed modulator ensured the construction of a sensor based on direct laser absorption spectroscopy, applying the QC laser with spectral characteristics matched to absorption lines of the detected substances. It can also be used in optical ranging and recognition systems.

Keywords: quantum cascade laser; laser controller; infrared modulator; laser spectroscopy; free space optics

1. Introduction

Quantum cascade (QC) laser technology is a commonly used radiation source in many applications that operates in mid-and far-infrared wavelengths [1–3]. These lasers are mainly used in chemical sensing and spectroscopy, in which low noise and high stability of both the light power and spectra are required [4,5]. To this application, a special low-noise current driver and temperature stabilizing unit were constructed [6]. However, these lasers are also being used in other applications as a result of their features, e.g., high power, modulation bandwidth, direct current control, compact size, room-temperature operation, and operation in high transparent spectral ranges of the atmosphere. These features are important for telecommunication, security, and defense technologies [7,8].

Some research works of the modeling techniques used for a simulation of QC lasers have been conducted. Their main focus was to describe the physical processes in electron transport in multiple-quantum-well heterostructures to improve properties for operating temperature, efficiency, and spectral range [9].

What is more, some electrical equivalent circuits were also developed to simulate the laser operation, analyzing the laser electrical features and driving electronics. These works use an emulator of simulating electrical circuits without creating additional mathematical functions or numerical calculations [10]. It is not so computationally intensive and can be implemented in lasing structure optimization or an applied-level device.

Although a simulation model of a realistic circuit should consider five rate equations of quantum wells, three-level or two-level models with certain approximations have been

used [10–12]. Based on these models, the light-current characteristics of QC laser were analyzed. These simulations were limited to intensity modulation characteristics for a different ratio to the threshold current.

However, only a few papers describe a QC laser pulse response [13]. The obtained results were used to define the influence of different bias currents on the turn-on delay of the pulse current conversion to the light signal. During described simulations, no model of the current driving unit was applied. The results verification was based on data from other circuit models or numerical calculations. These can be critical for some aspects of applied science in which laser-based systems are analyzed.

QC lasers require a new class of pulse drivers because their operational characteristics are different from those of a laser diode [14]. These lasers need driving signals (current and voltage) of an order higher than those of a bipolar diode laser [15]. The high voltage results from the applied cascade construction, in which the energy of the emitted photons is multiplied by the number of stages (e.g., 30–50). It can reach 20 V or more. The applied intersubband transitions are characterized by a lower optical gain than the interband, requiring high supplying currents. Therefore, the threshold current density of QC lasers is more than one order higher than that of diode lasers [16]. These features represent a challenge when constructing a laser driver that can consider both current and voltage. In these devices, various methods are applied to connect the signals to the QC laser. The most popular is to design unique signal poles or sockets on the printed circuit board (PCB) to connect the pins of the laser housing, e.g., butterfly, transistor outline package (TO), high heat load housing (HHL), and others. However, in a short pulse transmission, the main issues are impedance matching and inductance minimization. However, the matching can be impossible, because laser impedance depends on its construction and fabrication, temperature, or level of driving current [17]. The most critical is its dynamic change during current switching.

The properties of QC laser modulator radiation are matched to its application. Most often, they concern a required shape and the power of the emitted light. In the case of gas sensing devices, the applied laser absorption spectroscopy (LAS) technique determines the optical signal shape. This shape has a form ranging from a simple pulse to complex waveforms. For example, a QC laser pulse with a time duration of 500 ns was used in an intra-pulsed tuned LAS to detect the spectra of nitrogen oxide (NO) and nitrous oxide (N_2O) at around 5.25486 μm and 4.52284 μm, respectively [18]. Shorter pulses are also used, for example, in cavity-enhanced absorption spectroscopy to detect ammonia (NH_3), with a QC laser emitting 50 ns pulses at 200 kHz frequency around 6.8 μm [19].

More complex optical signals are preferable in a tunable laser absorption spectroscopy (TLAS). To obtain scanning of an absorption line range, the QC laser spectra are tuned applying both current ramp signal and high-frequency wave. Many LAS setups use tunable QC lasers, e.g., direct absorption spectroscopy or wavelength modulation [20]. In these setups, IR modulators generated the current signal consisting of, for example, a slow ramp (10 Hz) and a sinusoid (8 kHz) [21].

A high rate of radiation modulation is the primary goal of IR modulator construction for free-space optics (FSO). Some experimental results with GHz- range modulation of QC lasers have been described. In those tests, some specific architectures of laser structure were used [22]. For example, a laser waveguide with a microstrip line ensured a modulation rate of up to 14 GHz [23]. However, a 'high speed' technology of QC lasers is underdeveloped. The modulation speeds up to 26.5 GHz were obtained using a special design QC laser placed on a cold finger with continuous-flow liquid nitrogen and driven with bias-tee and a microwave signal [24].

There are many other applications for which it is important to design a compact and low-power consumption IR modulator. For example, it could be used as an alarm beacon with optical signals detected at extended ranges, a jamming device to disorientate an incoming missile threat, or a light source for beam riding and ranging systems. There are only a few such devices described in the literature [25]. However, they can work in pulsed

mode with closed construction, allowing light pulse generation in strictly defined pulse configurations at the maximum repetition rate of 500 kHz.

This study describes an integrated IR pulsed modulator consisting of a QC laser structure and a current switching module. It ensured the generation of short light pulses (tens of ns) with a maximum frequency of 1 MHz, using direct wire bonding of the lasing structure and the current terminals. Various simulations of this configuration were performed considering different QC laser electrical parameters. Finally, the preliminary experiments were performed with the designed modulator. The obtained results provided experimental verification of, e.g., the influence of both QC laser parameters and the driving signal interface on the light pulses, determination of the electrical scheme of the QC laser, and the integrated modulator. In the future, this modulator can be installed in some standard housings, e.g., HHL, butterfly.

2. QC Compact Laser Modulator Design

A compact laser modulator was built using a laser switching high-speed iC-G30 iCSY HG20M module (iC-House Corporation, Bodenheim, Germany) and a laser structure designed at the Institute of Electron Technology (Warsaw, Poland) [26,27]. The module is equipped with six channels, providing a speed of up to 250 MHz, current pulses of up to 5 A (per channel), and an output voltage of 30 V. Its main capabilities are independent and simple voltage control of channel currents, parallel channel operation of up to 6 A (constant mode) and up to 30 A (pulsed mode), and thermal shutdown. The QC laser was designed to operate at room temperature. Its parameters and construction mean it can be mounted directly on the signal pole of the laser switching module without the need to use an extra cooling unit. The optical power and voltage vs. current characteristics of the laser and a picture of the integrated modulator are presented in Figure 1.
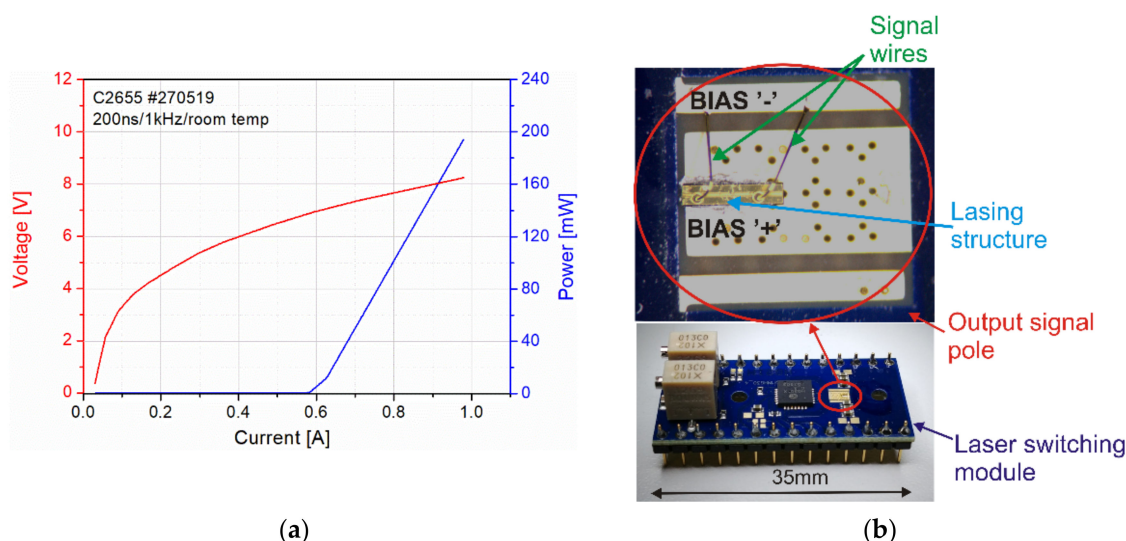

Figure 1. Optical power and voltage vs. current of the mounted QC laser (**a**) and a picture of the integrated IR modulator (**b**).

3. Simulations

The pulse operation performances of the laser modulator were analyzed using SPICE (Simulation Program with Integrated Circuit Emulation) models of the switching module and the prepared electrical model of the QC laser (LTSpice XVII software ver.17.0.27.0, Analog Devices, Norwood, MA, USA). During the simulations, no parameters for the PCB technology were included. Such assumptions simplify the scope of simulations but should be considered in actual conditions [28]. Its manufacturer delivered the SPICE description of the switching module. For the QC laser, the SPICE model was prepared using data from Alpes Lasers (St Blaise, Switzerland) for the lasing structure, and IXYS Corporation (Milpitas, CA, USA) for the inductance of the laser package [29,30]. In Figure 2, an electrical

schematic of the IR lighting device is presented. The Alpes laser model combines a resistor (R_L) and two capacitors (C_1, C_2). The R_L values depend on the laser operation point (e.g., for a low current: 10–20 Ω, and for the lasing current: 1–3 Ω). The C_1 (~100 pF) and C_2 (below 100 pF) are mainly determined by bonding pads and laser mounting technologies, respectively. IXYS Corporation determines the inductance level (L) for various signal interface technologies applied in laser housings. For example, a connection of two points at a distance of 0.2 mm, with a copper wire 0.014 mm in diameter and a height of 0.06 mm, gives an inductance of 3.6 nH.
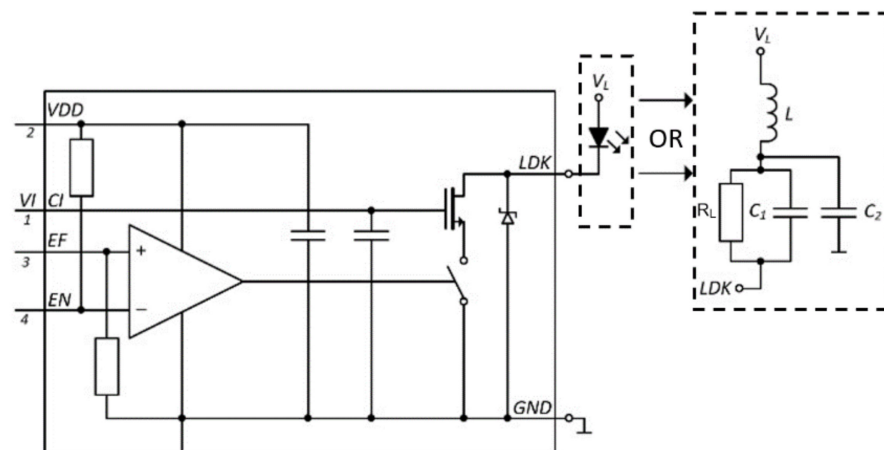

Figure 2. Electrical scheme of the IR modulator (V_{DD}—voltage supply of the module, *VI* (*CI*)—voltage control of output current, *EF-EN*—differential triggering signals).

A simulation of the light device was performed for different lasing structure electrical parameters (Figure 3). The reactance parts of load impedance did not influence the pulse amplitude (Figure 3a,b). The capacitances generate some oscillations at the pulse rising edge caused by feedback signals conditions. Growing these capacitances, the response time constant also increases. The most critical issue is load inductance, considering pulse shape and its oscillations. We observed a slower modulator response and current high-level changes for both biasing ranges. A current-voltage dependence for the inductor and signal resonance conditions defined these effects. Even at the rising and falling parts of the pulse, these signal fluctuations can be the critical point for the current amplitude, causing, e.g., laser structure damage. The bonding pad capacitance is an almost ideal plate capacitor with a PTFE dielectric [31]. For inductance, the bonding wire generally is 1 nH/mm. However, all of these parameters vary from laser to laser. To reduce pulse degradation, i.e., overshoot and ringing, any unnecessary hardware between the switching unit and the laser must be avoided. That is why the laser's direct and short connection to the electronics is preferable [32].

The load resistance has a direct influence on current amplitude and response time constant (Figure 3c). High resistance attenuates signal fluctuations at the pulse rising edge and increases its fall time. The current level is inversely proportional to this resistance. This is a crucial issue with regard to QCL's switching with dynamic resistance. There is a need to supply lasing structure to ensure population inversion (high resistance—low current—no light) and to emit photons (low resistance—high current—light) [33].
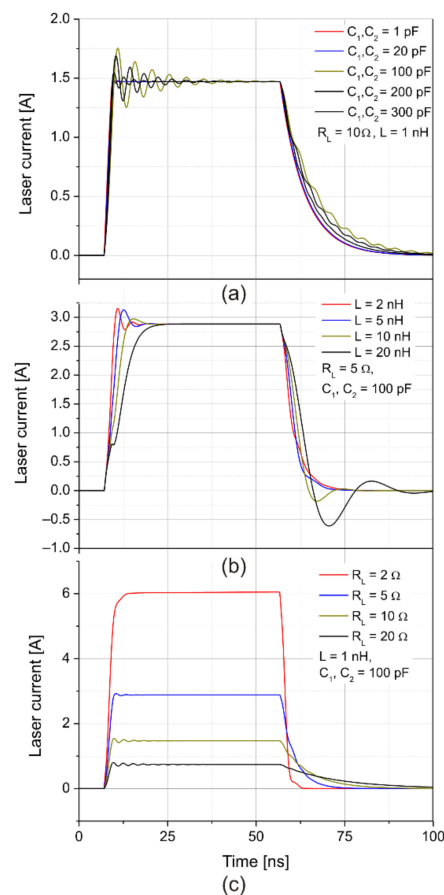
Figure 3. Simulation results of the modulator for different lasing structure electrical parameters: capacitance (**a**), inductance (**b**), and resistance (**c**).

4. Tests of the Laser Switching Module

The switching module tests were performed to analyze the influence of the load resistance on the shapes of the generated current pulses from the switching module using a special test board. The electrical signals were registered using the same scope Tektronix MSO 6 with the current probe CT-1 and the active differential voltage TDP-1500 probe. Figure 4 presents both the current and voltage signals for the two load resistances. These resistances were measured using a Keithley 236 source-measure unit. The module was operating in the current source region, where the current depends only on the 'load' of the biasing voltage. In this region, its output resistance is lower than 300 mΩ.
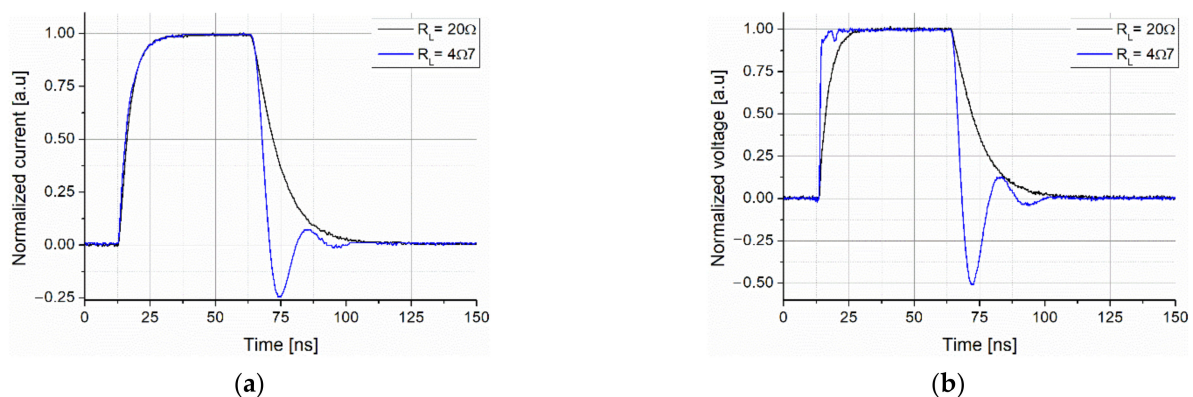

Figure 4. Normalized electrical driving signals: current (**a**) and voltage (**b**).

We observed both voltage and current oscillations at the falling slope for low load resistance. Impedance mismatching caused the transmission and reflection effects in the signal line. An increase in load resistance allowed for the minimizing of these effects with the limited bandwidth.

The load resistance influenced both edges of the voltage signals, but for the current, that was only noticed for the falling one. These differences can modulate the lasing conditions of the QC structure as determined by both current and voltage signals. In practice, these conditions are difficult to predict because they are related to the change in the QC laser impedance during its operation. Therefore, both the signal interface and QC laser parameters form the shapes of the light pulses.

5. Laboratory Tests of the IR Modulator

The preliminary tests of the IR modulator were performed using the lab setup presented in Figure 5. The modulator was placed on the test board to supply all signals (the voltage supply of the switching module, the differential triggering signals, and the biasing of the QC laser). The device was switched using the AFG 3252 model generator (Tektronix, Beaverton, OR, USA). The light pulses were registered with the PVI-4TE-10.6 (VIGO System S.A., Warsaw, Poland) detection module with a responsivity of 2.5×10^4 V/W and bandwidth of 500 MHz. An oscilloscope of the MSO 6 model (Tektronix) with the active probe (TDP-1500, Tektronix) visualized the voltage biasing of the laser structure. There was no technical possibility of registering current pulses (the laser wire was directly bonded on the driver signal pole) and analyzing their shapes.
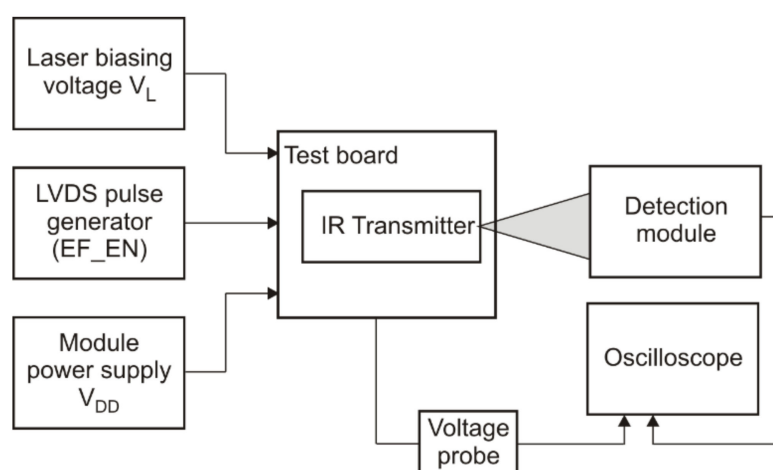
Figure 5. View of the testing setup and lasing device placed on the test board irradiating detection module.

Figure 6 presents some shapes of the registered voltage signals and radiation pulses for different pulse time durations at a frequency of 1 MHz. The voltage signal came ~5 ns faster than the light one, and the laser biasing voltage limited its amplitude. It agrees strongly with the data described in [28].

Some fluctuations caused by impedance mismatching of the signal interface were also observed. The high similarity of the shape of voltage signals obtained during reference measurements using a resistor (Figure 4b) and the QC laser is notable. But these shapes differed from those of the light pulses. A slower rising edge and laser pulse oscillations were noticed.
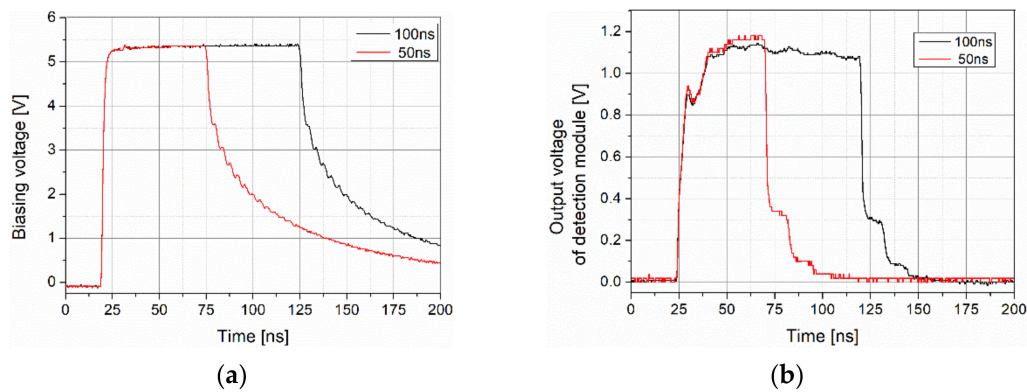
Figure 6. Registered signals for different pulse durations: biasing voltage (**a**) and radiation pulses (**b**).

Some virtues of the experimental and simulation results are shared, e.g., inflection in the rising slope, oscillations at the top signal, and some peaks at the falling edge (Figure 7). These effects were not registered for the tests with resistances, indicating that their source is a powered laser structure. This is a new aspect for analyses of QC laser module construction for applied science. Experimental results of laser biasing voltage and light pulse also defined the time delay of ~5 ns. This phenomenon was analyzed during modulation simulations.
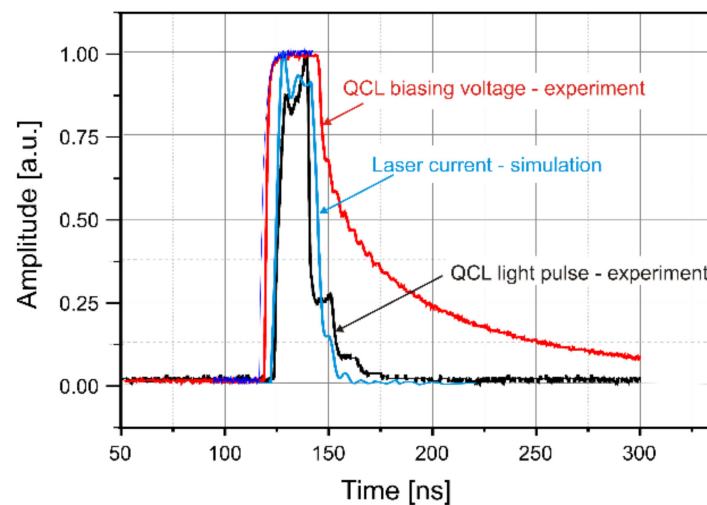

Figure 7. Comparison of experimental results (laser biasing voltage and light pulse) with simulation results (laser current).

6. Conclusions

This study presents the preliminary test of an integrated IR modulator. A unique characteristic of this study was the simulation of the electrical signals supplying the quantum cascade lasers, and the integration of the lasing structure and the current switching module. For this purpose, an electric circuit for the lasing structure was proposed. The simulated results defined the influence of impedance mismatching on both the current and voltage supply signals. It was shown that both signal interfaces and laser parameters form the shape of light pulses. The QCL impedance has non-Ohmic character. That is why it requires more advanced models to describe the behavior of the laser. A perfect impedance match is also impossible, because the QCL impedance changes with the modulation of the driving signal.

Finally, the integrated IR modulator was constructed. The shapes of its light pulses were comparable to the driving current obtained during simulations. These results confirm

the phenomenon of dynamic changes in QC laser impedance with current pulse duration. The electrical circuit emulation does not ensure the observation of these results. However, they provide new knowledge in the field of modeling QC lasing structures considering the laser-system approach.

The practical result of the work is an IR modulator that generates MWIR pulses using a QC laser operated at room temperature. The light time parameters, time duration of few tens of ns and max. frequency of 1 MHz, are unique results considering the performance of the other available compact QC laser modules.

Theoretically, the applied switching module also provides a bandwidth of 250 MHz and the generation of complex waveforms using six independently controlled current signals of up to 5 A, and a biasing voltage of 30 V. In the future, it will give new opportunities for many advanced applications. Such a modulator with combined optical signals is needed, e.g., in tunable direct laser absorption spectroscopy, multi-level optical signal transmission, and ultra-short pulse generation with a pre-biasing current.

References

1. Pecharroman-Gallego, R. An overview on quantum cascade lasers: Origins and development. In *Quantum Cascade Lasers*; Stavrou, V.N., Ed.; InTech: London, UK, 2017; pp. 1–24. [CrossRef]
2. Patel, C.K.N.; Lyakh, A.; Maulini, R.; Tsekoun, A.; Tadjikov, B. QCL as a game changer in MWIR and LWIR military and homeland security applications. *SPIE Proc.* **2012**, *8373*, 1–9. [CrossRef]
3. Bielecki, Z.; Stacewicz, T.; Wojtas, J.; Mikołajczyk, J. Application of quantum cascade lasers to trace gas detection. *Bull. Polish Acad. Sci. Tech. Sci.* **2015**, *63*, 515–525. [CrossRef]
4. Schwaighofer, A.; Brandstetter, M.; Lendl, B. Quantum cascade lasers (QCLs) in biomedical spectroscopy. *Chem. Soc. Rev.* **2017**, *46*, 5903–5924. [CrossRef] [PubMed]
5. Tombez, L.; Schilt, S.; Di Francesco, J.; Führer, T.; Rein, B.; Walther, T.; Di Domenico, G.; Hofstetter, D.; Thomann, P. Linewidth of a quantum-cascade laser assessed from its frequency noise spectrum and impact of the current driver. *Appl. Phys. B* **2012**, *109*, 407–414. [CrossRef]
6. Taubman, M.S. Low-noise high-performance current controllers for quantum cascade lasers. *Rev. Sci. Instrum.* **2011**, *82*, 1–8. [CrossRef]
7. Grasso, R.J. Defence and security applications of quantum cascade lasers. *SPIE Proc.* **2016**, *99330*, 1–12. [CrossRef]
8. Mikołajczyk, J. An overview of free space optics with quantum cascade lasers. *Int. J. Electron. Telecommun.* **2014**, *60*, 259–264. [CrossRef]
9. Jirauschek, C.; Kubis, T. Modeling techniques for quantum cascade lasers. *Appl. Phys. Rev.* **2014**, 1. [CrossRef]
10. Yong, K.; Haldar, M.; Webb, J.F. An equivalent circuit for quantum cascade lasers. *J. Infrared Milli Terahz Waves* **2013**, *34*. [CrossRef]
11. Donovan, K.; Harrison, P.; Kelsall, R.W. Self-consistent solutions to the intersubband rate equations in quantum cascade lasers: Analysis of a GaAs/AlxGa1−xAs device. *J. Appl. Phys.* **2001**, *89*, 3084. [CrossRef]
12. Darman, M.; Fasihi, K. Circuit-level modeling of quantum cascade lasers: Influence of Kerr effect on static and dynamic responses. *Optik* **2016**, *127*, 10303–10310. [CrossRef]

13. Chen, G.C.; Fan, G.H.; Li, S.T. Spice simulation of a large-signal model for quantum cascade laser. *Opt. Quant Electron.* **2008**, *40*, 645–653. [CrossRef]

14. Lindquist, J.R. Laser Drivers: Using a Laser Diode or Quantum-Cascade Laser? Don't Forget the Electronics. Laser Focus World 2018. Available online: https://digital.laserfocusworld.com/laserfocusworld/201806/MobilePagedArticle.action?articleId=1404129#articleId1404129 (accessed on 12 March 2021).

15. Zhang, Y.G.; Gu, Y.; Li, Y.Y.; Li, A.Z.; Li, C.; Cao, Y.Y.; Zhou, L. An effective TDLS setup using homemade driving modules for evaluation of pulsed QCL. *Appl. Phys. B* **2012**, *109*, 541–548. [CrossRef]

16. Tournié, E.; Baranov, A.N. Mid-infrared semiconductor lasers: A review. In *Semiconductors and Semimetals*; Coleman, J.J., Bryce, A.C., Jagadishm, C., Eds.; Elsevier: Amsterdam, The Netherlands, 2012; Volume 86, pp. 183–226. [CrossRef]

17. Ashok, P.; Ganesh, M. Impedance characteristics of mid infra red quantum cascade lasers. *Opt. Laser Technol.* **2021**, *134*. [CrossRef]

18. Douat, C.; Hübner, S.; Engeln, R.; Benedikt, J. Production of nitric/nitrous oxide by an atmospheric pressure plasma jet. *Plasma Sources Sci. Technol.* **2016**, 25. [CrossRef]

19. Gadedjisso-Tossou, K.S.; Stoychev, L.I.; Mohou, M.A.; Cabrera, H.; Niemela, J.; Danailov, M.B.; Vacchi, A. Cavity ring-down spectroscopy for molecular trace gas detection using a pulsed DFB QCL emitting at 6.8 µm. *Photonics* **2020**, *7*, 74. [CrossRef]

20. Bolshov, M.A.; Kuritsyn Yu, A.; Romanovskii Yu, V. Tunable diode laser spectroscopy as a technique for combustion diagnostics. *Spectrochim. Acta Part B At. Spectrosc.* **2015**, *106*, 45–66. [CrossRef]

21. Upadhyay, A.; Wilson, D.; Lengden, M.; Chakraborty, A.L.; Stewart, G.; Johnstone, W. Calibration-free WMS using a cw-DFB-QCL, a VCSEL, and an Edge-emitting DFB laser with in-situ real-time laser parameter characterization. *IEEE Photonics J.* **2017**, *9*. [CrossRef]

22. Pirotta, S.; Tran, N.-L.; Jollivet, A.; Biasiol, G.; Crozat, P.; Manceau, J.-M.; Bousseksou, A.; Colombelli, R. Fast amplitude modulation up to 1.5 GHz of mid-IR free-space beams at room-temperature. *Nat. Commun.* **2021**, *12*. [CrossRef]

23. St-Jean, M.R.; Amanti, M.I.; Bernard, A.; Calvar, A.; Bismuto, A.; Gini, E.; Beck, M.; Faist, J.; Liu, H.C.; Sirtori, C. Injection locking of mid-infrared quantum cascade laser at 14 GHz, by direct microwave modulation. *Laser Photonics Rev.* **2014**, *8*, 443–449. [CrossRef]

24. Mottaghizadeh, A.; Asghari, Z.; Amanti, M.; Gacemi, D.; Vasanelli, A.; Sirtori, C. Ultra-fast modulation of mid infrared buried heterostructure quantum cascade lasers. In Proceedings of the 42nd International Conference on Infrared, Millimeter, and Terahertz Waves (IRMMW-THz), Cancun, Mexico, 27 August–1 September 2017. [CrossRef]

25. iC-HN iCSY HN1M High-Speed Module. Available online: https://www.ichaus.de/upload/pdf/HN1M_evalmanual_A3en.pdf (accessed on 30 June 2021).

26. Pierściński, K.; Pierścińska, D.; Kuźmicz, A.; Sobczak, G.; Bugajski, M.; Gutowski, P.; Chmielewski, K. Coupled cavity Mid-IR quantum cascade lasers fabricated by dry etching. *Photonics* **2020**, *7*, 45. [CrossRef]

27. Electrical Model. Available online: https://www.alpeslasers.ch/?a=36,41 (accessed on 30 June 2021).

28. Yang, K.; Liu, J.; Zhai, S.; Zhang, J.; Zhuo, N.; Wang, L.; Liu, S.; Liu, F. Room-temperature quantum cascade laser packaged module at ∼8 µm designed for high-frequency response. *Electron. Lett.* **2021**, 1–3. [CrossRef]

29. PCO-7120 Laser Diode Driver Module. Available online: https://ixapps.ixys.com/DataSheet/pco-7120_manual.pdf (accessed on 30 June 2021).

30. Ashok, P.; Ganesh, M. Optimum electrical pulse characteristics for efficient gain switching in QCL. *Optik* **2017**, *146*, 51–62. [CrossRef]

31. Hemingway, M. External Cavity Quantum Cascade Lasers. Ph.D. Thesis, University of Sheffield, Sheffield, UK, 2018.

32. Gwinner, S. How to Choose a Pulsed Laser Diode Driver. Available online: https://www.laserdiodecontrol.com/How-to-Choose-a-Pulsed-Laser-Diode-Driver (accessed on 30 June 2021).

33. Mikołajczyk, J. Data Link with a High-Power Pulsed Quantum Cascade Laser Operating at the Wavelength of 4.5 µm. *Sensors* **2021**, *21*, 3231. [CrossRef] [PubMed]